

Shape Reconstruction in Linear Elasticity: Standard and Linearized Monotonicity Method

Sarah Eberle and Bastian Harrach

Institute of Mathematics, Goethe-University Frankfurt, Frankfurt am Main, Germany

E-mail: eberle@math.uni-frankfurt.de, harrach@math.uni-frankfurt.de

Abstract. In this paper, we deal with the inverse problem of the shape reconstruction of inclusions in elastic bodies. The main idea of this reconstruction is based on the monotonicity property of the Neumann-to-Dirichlet operator presented in a former article of the authors. Thus, we introduce the so-called standard as well as linearized monotonicity tests in order to detect and reconstruct inclusions. In addition, we compare these methods with each other and present several numerical test examples.

Keywords: linear elasticity, inverse problem, shape reconstruction, monotonicity method

1. Introduction and problem statement

The reconstruction of inclusions in materials by nondestructive testing becomes more and more important and opens a wide mathematical field in inverse problems. The applications cover engineering, geoscientific and medical problems. This is the reason, why several authors dealt with the inverse problem of linear elasticity in order to recover the Lamé parameters. For the two dimensional case, we refer the reader to [15, 20, 16, 18]. Further on, in three dimensions, [21, 22] and [5] gave the proof for uniqueness results for both Lamé coefficients under the assumption that μ is close to a positive constant. [1, 2] proved the uniqueness for partial data, where the Lamé parameters are piecewise constant and some boundary determination results were shown in [19, 21, 18].

In this paper, the key issue of the shape reconstruction of inclusions is the monotonicity property of the corresponding Neumann-to-Dirichlet operator (see [23, 24]). These monotonicity properties were also applied for electrical impedance tomography (see, e.g., [13]) and for linear elasticity in [4], which is the basis for our current work. Our approach relies on the monotonicity of the Neumann-to-Dirichlet operator with respect to the Lamé parameters and the techniques of localized potentials [12, 11, 9, 7, 8].

Thus, we start with the introduction of the problem and summarize the main results from [4]. After that, we go over to the shape reconstruction itself, where we consider the standard and linearized monotonicity method. In doing so, we present and compare numerical experiments from the aforementioned two methods.

We start with the introduction of the problem of interest in the following way. We consider a bounded and connected open set $\Omega \subset \mathbb{R}^d$ ($d = 2$ or 3), occupied by an isotropic material with linear stress-strain relation, where Γ_D and Γ_N with $\Gamma_D \cup \Gamma_N = \partial\Omega$ are the corresponding Dirichlet and Neumann boundaries. Then the displacement vector $u : \bar{\Omega} \rightarrow \mathbb{R}^d$ satisfies the boundary value problem

$$\begin{cases} -\mu\Delta u - (\lambda + \mu)\nabla(\nabla \cdot u) = 0 & \text{in } \Omega, \\ \left(\lambda(\nabla \cdot u)I + 2\mu\hat{\nabla}u \right) n = g & \text{on } \Gamma_N, \\ u = 0 & \text{on } \Gamma_D, \end{cases} \quad (1)$$

where μ, λ are the Lamé parameters, $\hat{\nabla}u = \frac{1}{2}(\nabla u + (\nabla u)^T)$ is the symmetric gradient, n is the normal vector pointing outside of Ω , $g \in L^2(\Gamma_N)^d$ the boundary load and I the $d \times d$ -identity matrix.

For given constants $\alpha_1, \alpha_2, \beta_1, \beta_2$ satisfying $0 < \alpha_1 \leq \alpha_2$, $0 < \beta_1 \leq \beta_2$, we define the set of admissible Lamé parameters by

$$\mathcal{A} = \{(\lambda, \mu) : (\lambda, \mu) \in L^\infty(\Omega) \times C^{0,1}(\Omega), \alpha_1 \leq \lambda \leq \alpha_2, \beta_1 \leq \mu \leq \beta_2\}.$$

The weak formulation of the problem (1) is given by

$$\int_{\Omega} 2\mu \hat{\nabla}u : \hat{\nabla}v + \lambda \nabla \cdot u \nabla \cdot v \, dx = \int_{\Gamma_N} g \cdot v \, ds \quad \text{for all } v \in \mathcal{V}, \quad (2)$$

where

$$\mathcal{V} := \left\{ v \in H^1(\Omega)^d : v|_{\Gamma_D} = 0 \right\}.$$

We want to remark that in continuum mechanics, the function v from the test space \mathcal{V} can be seen as a virtual displacement, while the weak formulation (2) itself can be interpreted as the principle of virtual work.

The existence and uniqueness of a solution to the above variational formulation (2) follows from the Lax-Milgram theorem, see e.g., in [3].

For the sake of completeness, we state two important inequalities (see e.g., [6]) in the framework of elasticity, which play an essential role in the proof of the aforementioned existence and uniqueness of the solution of the weak formulation.

Korn's first inequality:

Let Ω be a bounded and connected open set in \mathbb{R}^d . Then, there exists a constant c such that

$$c\|v\|_{H^1(\Omega)^d} \leq \|\hat{\nabla}v\|_{L^2(\Omega)^{d \times d}} \quad \text{for all } v \in \mathcal{V}.$$

Korn's second inequality:

Let Ω be a bounded and connected open set in \mathbb{R}^d . Then there exists a constant c such that

$$c\|v\|_{H^1(\Omega)^d} \leq \|\hat{\nabla}v\|_{L^2(\Omega)^{d \times d}} + \|v\|_{L^2(\Omega)^d} \quad \text{for all } v \in \mathcal{V}.$$

Next, we introduce the Neumann-to-Dirichlet operator $\Lambda(\lambda, \mu)$ by

$$\Lambda(\lambda, \mu) : L^2(\Gamma_N)^d \rightarrow L^2(\Gamma_N)^d : g \mapsto u|_{\Gamma_N}.$$

It is well known that $\Lambda(\lambda, \mu)$ is a self-adjoint compact linear operator. The associated bilinear form is given by

$$\langle g, \Lambda(\lambda, \mu)h \rangle = \int_{\Omega} 2\mu \hat{\nabla} u_{(\lambda, \mu)}^{(g)} : \hat{\nabla} u_{(\lambda, \mu)}^{(h)} + \lambda \nabla \cdot u_{(\lambda, \mu)}^{(g)} \nabla \cdot u_{(\lambda, \mu)}^{(h)} dx,$$

where $u_{(\lambda, \mu)}^{(g)}$ solves the elastic problem (1) and $u_{(\lambda, \mu)}^{(h)}$ the corresponding problem with boundary load h .

The operator $\Lambda(\lambda, \mu)$ is Fréchet differentiable, which can be proven by similar arguments as in the corresponding proof in [17] for the impedance tomography problem.

For directions $\hat{\lambda}, \hat{\mu} \in L^\infty(\Omega)$, the derivative

$$\Lambda'(\lambda, \mu)(\hat{\lambda}, \hat{\mu}) : L^2(\Gamma_N)^d \rightarrow L^2(\Gamma_N)^d$$

is the self-adjoint compact linear operator associated to the bilinear form so that

$$\begin{aligned} \langle \Lambda'(\lambda, \mu)(\hat{\lambda}, \hat{\mu})g, h \rangle & \\ &= - \int_{\Omega} 2\hat{\mu} \hat{\nabla} u_{(\lambda, \mu)}^{(g)} : \hat{\nabla} u_{(\lambda, \mu)}^{(h)} + \hat{\lambda} \nabla \cdot u_{(\lambda, \mu)}^{(g)} \nabla \cdot u_{(\lambda, \mu)}^{(h)} dx. \end{aligned} \quad (3)$$

Note that for $\hat{\lambda}_0, \hat{\lambda}_1, \hat{\mu}_0, \hat{\mu}_1 \in L^\infty(\Omega)$, we obviously have that for

$$\hat{\lambda}_0 \leq \hat{\lambda}_1 \text{ and } \hat{\mu}_0 \leq \hat{\mu}_1$$

it follows that

$$\Lambda'(\lambda, \mu)(\hat{\lambda}_0, \hat{\mu}_0) \geq \Lambda'(\lambda, \mu)(\hat{\lambda}_1, \hat{\mu}_1).$$

Remark 1.1 *The inverse problem we consider here is the following:*

Find (λ, μ) knowing the Neumann-to-Dirichlet operator $\Lambda(\lambda, \mu)$.

2. Monotonicity methods

In this section, we introduce two monotonicity methods in order to reconstruct inclusions in elastic bodies. The first method is the standard (or non-linearized) monotonicity method and the second the linearized monotonicity method. For both methods, we analyze the monotonicity properties for the Neumann-to-Dirichlet operator and formulate the corresponding monotonicity test which we apply for the realization of the numerical experiments.

First, we summarize and present the required results concerning the monotonicity properties. The details and proofs can be found in [4]. We start with the monotonicity estimate and the monotonicity property itself, which is the key issue for our study and will be analyzed later on in detail.

Lemma 2.1 (Lemma 3.1 from [4]) Let $(\lambda_0, \mu_0), (\lambda_1, \mu_1) \in \mathcal{A}$, $g \in L^2(\Gamma_N)^d$ be an applied boundary load, and let $u_0 := u_{(\lambda_0, \mu_0)}^{(g)} \in \mathcal{V}$, $u_1 := u_{(\lambda_1, \mu_1)}^{(g)} \in \mathcal{V}$. Then

$$\int_{\Omega} 2(\mu_0 - \mu_1) \hat{\nabla} u_1 : \hat{\nabla} u_1 + (\lambda_0 - \lambda_1) \nabla \cdot u_1 \nabla \cdot u_1 \, dx \quad (4)$$

$$\begin{aligned} &\geq \langle g, \Lambda(\lambda_1, \mu_1)g \rangle - \langle g, \Lambda(\lambda_0, \mu_0)g \rangle \\ &\geq \int_{\Omega} 2(\mu_0 - \mu_1) \hat{\nabla} u_0 : \hat{\nabla} u_0 + (\lambda_0 - \lambda_1) \nabla \cdot u_0 \nabla \cdot u_0 \, dx. \end{aligned} \quad (5)$$

Lemma 2.2 Let $(\lambda_0, \mu_0), (\lambda_1, \mu_1) \in \mathcal{A}$, $g \in L^2(\Gamma_N)^d$ be an applied boundary load, and let $u_0 := u_{(\lambda_0, \mu_0)}^{(g)} \in \mathcal{V}$, $u_1 := u_{(\lambda_1, \mu_1)}^{(g)} \in \mathcal{V}$. Then

$$\langle g, \Lambda(\lambda_1, \mu_1)g \rangle - \langle g, \Lambda(\lambda_0, \mu_0)g \rangle \quad (6)$$

$$\begin{aligned} &\geq \int_{\Omega} 2 \left(\mu_1 - \frac{\mu_1^2}{\mu_0} \right) \hat{\nabla} u_1 : \hat{\nabla} u_1 \, dx + \int_{\Omega} \left(\lambda_1 - \frac{\lambda_1^2}{\lambda_0} \right) \nabla \cdot u_1 \nabla \cdot u_1 \, dx \\ &= \int_{\Omega} 2 \frac{\mu_1}{\mu_0} (\mu_0 - \mu_1) \hat{\nabla} u_1 : \hat{\nabla} u_1 \, dx + \int_{\Omega} \frac{\lambda_1}{\lambda_0} (\lambda_0 - \lambda_1) \nabla \cdot u_1 \nabla \cdot u_1 \, dx. \end{aligned} \quad (7)$$

Proof We start with a result shown in the poof of Lemma 3.1 in [4]:

$$\begin{aligned} &\langle g, \Lambda(\lambda_1, \mu_1)g \rangle - \langle g, \Lambda(\lambda_0, \mu_0)g \rangle \\ &= \int_{\Omega} 2\mu_1 \hat{\nabla} (u_1 - u_0) : \hat{\nabla} (u_1 - u_0) + \lambda_1 \nabla \cdot (u_1 - u_0) \nabla \cdot (u_1 - u_0) \\ &\quad + 2(\mu_0 - \mu_1) \hat{\nabla} u_0 : \hat{\nabla} u_0 + (\lambda_0 - \lambda_1) \nabla \cdot u_0 \nabla \cdot u_0 \, dx. \end{aligned}$$

Based on this, we are led to

$$\begin{aligned} &\langle g, \Lambda(\lambda_1, \mu_1)g \rangle - \langle g, \Lambda(\lambda_0, \mu_0)g \rangle \\ &= \int_{\Omega} 2\mu_1 \hat{\nabla} u_1 : \hat{\nabla} u_1 - 4\mu_1 \hat{\nabla} u_1 : \hat{\nabla} u_0 + 2\mu_1 \hat{\nabla} u_0 : \hat{\nabla} u_0 + \lambda_1 \nabla \cdot u_1 \nabla \cdot u_1 \\ &\quad - 2\lambda_1 \nabla \cdot u_1 \nabla \cdot u_0 + \lambda_1 \nabla \cdot u_0 \nabla \cdot u_0 + 2\mu_0 \hat{\nabla} u_0 : \hat{\nabla} u_0 + \lambda_0 \nabla \cdot u_0 \nabla \cdot u_0 \\ &\quad - 2\mu_1 \hat{\nabla} u_0 : \hat{\nabla} u_0 - \lambda_1 \nabla \cdot u_0 \nabla \cdot u_0 \, dx \\ &= \int_{\Omega} 2\mu_1 \left| \hat{\nabla} u_1 \right|^2 - 4\mu_1 \hat{\nabla} u_1 : \hat{\nabla} u_0 + \lambda_1 \left| \nabla \cdot u_1 \right|^2 - 2\lambda_1 \nabla \cdot u_1 \nabla \cdot u_0 \\ &\quad + 2\mu_0 \left| \hat{\nabla} u_0 \right|^2 + \lambda_0 \left| \nabla \cdot u_0 \right|^2 \, dx \\ &= \int_{\Omega} 2\mu_0 \left| \hat{\nabla} u_0 - \frac{\mu_1}{\mu_0} \hat{\nabla} u_1 \right|^2 + \lambda_0 \left| \nabla \cdot u_0 - \frac{\lambda_1}{\lambda_0} \nabla \cdot u_1 \right|^2 \\ &\quad + \left(2\mu_1 - \frac{2\mu_1^2}{\mu_0} \right) \left| \hat{\nabla} u_1 \right|^2 + \left(\lambda_1 - \frac{\lambda_1^2}{\lambda_0} \right) \left| \nabla \cdot u_1 \right|^2 \, dx \\ &\geq \int_{\Omega} 2 \left(\mu_1 - \frac{\mu_1^2}{\mu_0} \right) \left| \hat{\nabla} u_1 \right|^2 + \left(\lambda_1 - \frac{\lambda_1^2}{\lambda_0} \right) \left| \nabla \cdot u_1 \right|^2 \, dx. \end{aligned}$$

□

Lemma 2.2 leads directly to

Corollary 2.1 (Corollary 3.2 from [4]) For $(\lambda_0, \mu_0), (\lambda_1, \mu_1) \in \mathcal{A}$

$$\lambda_0 \leq \lambda_1 \text{ and } \mu_0 \leq \mu_1 \text{ implies } \Lambda(\lambda_0, \mu_0) \geq \Lambda(\lambda_1, \mu_1).$$

Based on these results, we can go over to the standard monotonicity method.

2.1. Standard monotonicity method

Our aim is to prove that the opposite direction of Corollary 2.1 holds true in order to formulate the so-called standard monotonicity test (Corollary 2.2 and 2.3).

Therefore, we consider the case where Ω contains inclusions in which the Lamé parameters λ and μ differ from otherwise known background Lamé parameters.

For the precise formulation, we will now introduce the concept of the inner and the outer support of a measurable function in a similar way as in [13].

Definition 2.1 *A relatively open set $U \subseteq \bar{\Omega}$ is called connected to $\partial\Omega$ if $U \cap \Omega$ is connected and $U \cap \partial\Omega \neq \emptyset$.*

Definition 2.2 *For a measurable function $\varphi : \Omega \rightarrow \mathbb{R}^2$, we define*

- a) *the support $\text{supp}(\varphi)$ as the complement (in $\bar{\Omega}$) of the union of those relatively open $U \subseteq \bar{\Omega}$, for which $\varphi|_U \equiv 0$,*
- b) *the inner support $\text{inn supp}(\varphi)$ as the union of those open sets $U \subseteq \Omega$, for which $\text{ess inf}_{x \in U} \|\varphi(x)\| > 0$,*
- c) *the outer support $\text{out}_{\partial\Omega} \text{supp}(\varphi)$ as the complement (in $\bar{\Omega}$) of the union of those relatively open $U \subseteq \bar{\Omega}$ that are connected to $\partial\Omega$ and for which $\varphi|_U \equiv 0$.*

For ease of notations, we assume that the background Lamé parameters are equal to (λ_0, μ_0) . Further on, we consider $\varphi = (\lambda - \lambda_0, \mu - \mu_0)^T$. Our goal is to determine the inclusion

$$\mathcal{D} := \text{out}_{\partial\Omega} \text{supp}(\varphi) \tag{8}$$

from the knowledge of the Neumann-to-Dirichlet operator $\Lambda(\lambda, \mu)$. Hence, the inclusion in our nomenclature always contains the support of φ as well as all holes which cannot be connected to the boundary.

Let us consider the setting (8) as depicted in Figure 1. By proving the opposite direction of Corollary 2.1, we show that \mathcal{D} can be reconstructed by monotonicity tests, which simply compare $\Lambda(\lambda, \mu)$ (in the sense of quadratic forms) to the Neumann-to-Dirichlet operators $\Lambda(\lambda_1, \mu_1)$ of test parameters (λ_1, μ_1) . To be more precise, the support of φ can be reconstructed under the assumption that $\text{supp}(\varphi) \subset \Omega$ has a connected complement, in which case we have $\text{supp}(\varphi) = \text{out}_{\partial\Omega} \text{supp}(\varphi) = \mathcal{D}$ (c.f. [13]). Otherwise, what we can reconstruct is the support of φ together with all holes that have no connection to the boundary $\partial\Omega$, i.e. \mathcal{D} (c.f. [10]). Hence, in this paper we only take a look at inclusions with $\text{supp}(\varphi) = \text{out}_{\partial\Omega} \text{supp}(\varphi) = \mathcal{D}$.

This leads to the formulation of the standard monotonicity test which is implemented in the next part. In the following, we define α and β as the contrasts and $\chi_{\mathcal{D}}$ as well as $\chi_{\mathcal{B}}$ as the characteristic function w.r.t. the inclusion \mathcal{D} and the so-called test inclusion \mathcal{B} , respectively.

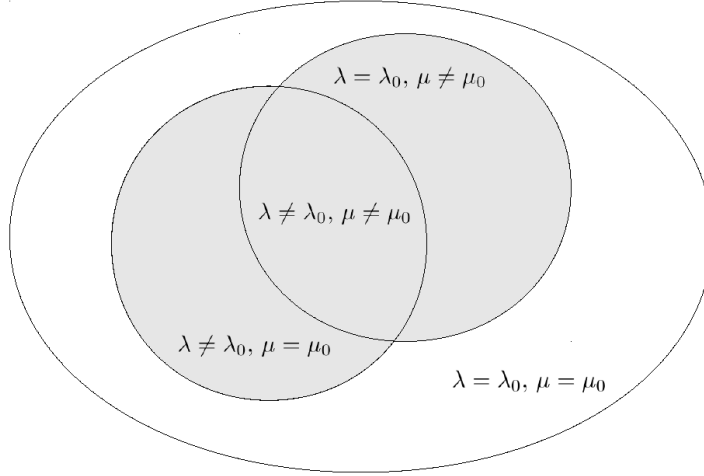


Figure 1. Exemplary $\text{out}_{\partial\Omega} \text{supp}(\varphi)$ for an inclusion without holes in gray.

Theorem 2.1 *Let $(\lambda, \mu) \in L^\infty(\Omega) \times C^{0,1}(\Omega)$ and $\lambda \geq \lambda_0, \mu \geq \mu_0$. For every open set \mathcal{B} (e.g. ball or cube) and every $\alpha, \beta \geq 0, \alpha + \beta > 0$,*

$$\alpha\chi_{\mathcal{B}} \leq \lambda - \lambda_0, \quad \beta\chi_{\mathcal{B}} \leq \mu - \mu_0$$

implies

$$\Lambda(\lambda_0 + \alpha\chi_{\mathcal{B}}, \mu_0 + \beta\chi_{\mathcal{B}}) \geq \Lambda(\lambda, \mu)$$

and

$$\mathcal{B} \not\subseteq \mathcal{D}$$

implies

$$\Lambda(\lambda_0 + \alpha\chi_{\mathcal{B}}, \mu_0 + \beta\chi_{\mathcal{B}}) \not\geq \Lambda(\lambda, \mu).$$

Hence, the set

$$R := \bigcup_{\alpha, \beta \geq 0, \alpha + \beta > 0} \{\mathcal{B} \subseteq \Omega : \Lambda(\lambda_0 + \alpha\chi_{\mathcal{B}}, \mu_0 + \beta\chi_{\mathcal{B}}) \geq \Lambda(\lambda, \mu)\},$$

fulfills

$$\text{inn supp}((\lambda - \lambda_0, \mu - \mu_0)^T) \subseteq R \subseteq \mathcal{D}.$$

Proof Let $(\lambda, \mu) \in L^\infty(\Omega) \times C^{0,1}(\Omega)$ and $\lambda \geq \lambda_0, \mu \geq \mu_0$. Let \mathcal{B} be an open set and $\alpha, \beta \geq 0, \alpha + \beta > 0$ and

$$\alpha\chi_{\mathcal{B}} \leq \lambda - \lambda_0, \quad \beta\chi_{\mathcal{B}} \leq \mu - \mu_0.$$

We start with Lemma 2.2 and get

$$\begin{aligned} & \langle g, \Lambda(\lambda_0 + \alpha\chi_{\mathcal{B}}, \mu_0 + \beta\chi_{\mathcal{B}})g \rangle - \langle g, \Lambda(\lambda, \mu)g \rangle \\ & \geq \int_{\Omega} 2 \frac{\mu_0 + \beta\chi_{\mathcal{B}}}{\mu} (\mu - \mu_0 - \beta\chi_{\mathcal{B}}) \hat{\nabla} u_{(\lambda_0 + \alpha\chi_{\mathcal{B}}, \mu_0 + \beta\chi_{\mathcal{B}})} : \hat{\nabla} u_{(\lambda_0 + \alpha\chi_{\mathcal{B}}, \mu_0 + \beta\chi_{\mathcal{B}})} \\ & \quad + \frac{\lambda_0 + \alpha\chi_{\mathcal{B}}}{\lambda} (\lambda - \lambda_0 - \alpha\chi_{\mathcal{B}}) \nabla \cdot u_{(\lambda_0 + \alpha\chi_{\mathcal{B}}, \mu_0 + \beta\chi_{\mathcal{B}})} \nabla \cdot u_{(\lambda_0 + \alpha\chi_{\mathcal{B}}, \mu_0 + \beta\chi_{\mathcal{B}})} dx. \end{aligned}$$

This shows that with $\lambda = \lambda_0 + (\lambda_1 - \lambda_0)\chi_{\mathcal{D}}$, $\mu = \mu_0 + (\mu_1 - \mu_0)\chi_{\mathcal{D}}$, the condition $\alpha\chi_{\mathcal{B}} \leq \lambda - \lambda_0$, $\beta\chi_{\mathcal{B}} \leq \mu - \mu_0$ implies

$$\langle g, \Lambda(\lambda_0 + \alpha\chi_{\mathcal{B}}, \mu_0 + \beta\chi_{\mathcal{B}})g \rangle - \langle g, \Lambda(\lambda, \mu)g \rangle \geq 0.$$

Hence, we get with Corollary 2.1 that

$$\Lambda(\lambda_0 + \alpha\chi_{\mathcal{B}}, \mu_0 + \beta\chi_{\mathcal{B}}) \geq \Lambda(\lambda, \mu).$$

It remains to show that

$$\mathcal{B} \not\subseteq \mathcal{D} \quad \text{implies} \quad \Lambda(\lambda_0 + \alpha\chi_{\mathcal{B}}, \mu_0 + \beta\chi_{\mathcal{B}}) \not\geq \Lambda(\lambda, \mu).$$

Let $\mathcal{B} \not\subseteq \mathcal{D}$. Corollary 2.1 states that shrinking the open set \mathcal{B} only makes $\Lambda(\lambda_0 + \alpha\chi_{\mathcal{B}}, \mu_0 + \beta\chi_{\mathcal{B}})$ larger, so that we can assume without loss of generality that $\mathcal{B} \subseteq \Omega \setminus \mathcal{D}$. We can apply Theorem 3.3 from [4] and obtain a sequence $(g_n)_{n \in \mathbb{N}} \subset L^2(\Gamma_{\mathbb{N}})^d$ so that the solutions $(u^{(g_n)})_{n \in \mathbb{N}} \subset \mathcal{V}$, of

$$\left\{ \begin{array}{l} -(\mu_0 + \beta\chi_{\mathcal{B}})\Delta u^{(g_n)} - ((\lambda_0 + \alpha\chi_{\mathcal{B}}) + (\mu_0 + \beta\chi_{\mathcal{B}}))\nabla(\nabla \cdot u^{(g_n)}) = 0 \quad \text{in } \Omega, \\ \left((\lambda_0 + \alpha\chi_{\mathcal{B}})(\nabla \cdot u^{(g_n)})I + 2(\mu_0 + \beta\chi_{\mathcal{B}})\hat{\nabla}u^{(g_n)} \right) n = g_n \quad \text{on } \Gamma_{\mathbb{N}}, \\ u^{(g_n)} = 0 \quad \text{on } \Gamma_{\mathbb{D}}, \end{array} \right. \quad (9)$$

fulfill

$$\lim_{n \rightarrow \infty} \int_{\mathcal{B}} \hat{\nabla}u^{(g_n)} : \hat{\nabla}u^{(g_n)} dx = \infty, \quad (10)$$

$$\lim_{n \rightarrow \infty} \int_{\mathcal{D}} \hat{\nabla}u^{(g_n)} : \hat{\nabla}u^{(g_n)} dx = 0, \quad (11)$$

$$\lim_{n \rightarrow \infty} \int_{\mathcal{B}} \nabla \cdot u^{(g_n)} \nabla \cdot u^{(g_n)} dx = \infty, \quad (12)$$

$$\lim_{n \rightarrow \infty} \int_{\mathcal{D}} \nabla \cdot u^{(g_n)} \nabla \cdot u^{(g_n)} dx = 0. \quad (13)$$

From Lemma 2.1 and Equation (10)-(13) it follows with $u^{(g_n)}$ as in system (9), $\mu = \mu_0 + (\mu_1 - \mu_0)\chi_{\mathcal{D}}$ and $\lambda = \lambda_0 + (\lambda_1 - \lambda_0)\chi_{\mathcal{D}}$, where the index 0 represents the reference medium and the index 1 indicates the parameters of the inclusion, that

$$\begin{aligned} & \langle g_n, \Lambda(\lambda_0 + \alpha\chi_{\mathcal{B}}, \mu_0 + \beta\chi_{\mathcal{B}}) - \Lambda(\lambda, \mu)g_n \rangle \\ &= \langle g_n, \Lambda(\lambda_0 + \alpha\chi_{\mathcal{B}}, \mu_0 + \beta\chi_{\mathcal{B}})g_n \rangle - \langle g_n, \Lambda(\lambda, \mu)g_n \rangle \\ &\leq \int_{\Omega} 2(\mu_0 + (\mu_1 - \mu_0)\chi_{\mathcal{D}})\hat{\nabla}u^{(g_n)} : \hat{\nabla}u^{(g_n)} \\ &\quad + (\lambda_0 + (\lambda_1 - \lambda_0)\chi_{\mathcal{D}})\nabla \cdot u^{(g_n)}\nabla \cdot u^{(g_n)} dx \\ &\quad - \int_{\Omega} 2(\mu_0 + \beta\chi_{\mathcal{B}})\hat{\nabla}u^{(g_n)} : \hat{\nabla}u^{(g_n)} + (\lambda_0 + \alpha\chi_{\mathcal{B}})\nabla \cdot u^{(g_n)}\nabla \cdot u^{(g_n)} dx \\ &= \int_{\Omega} 2(\mu_1 - \mu_0)\chi_{\mathcal{D}}\hat{\nabla}u^{(g_n)} : \hat{\nabla}u^{(g_n)} + (\lambda_1 - \lambda_0)\chi_{\mathcal{D}}\nabla \cdot u^{(g_n)}\nabla \cdot u^{(g_n)} \\ &\quad - 2\beta\chi_{\mathcal{B}}\hat{\nabla}u^{(g_n)} : \hat{\nabla}u^{(g_n)} - \alpha\chi_{\mathcal{B}}\nabla \cdot u^{(g_n)}\nabla \cdot u^{(g_n)} dx \end{aligned}$$

$$\begin{aligned}
&= - \int_{\mathcal{B}} 2\beta \hat{\nabla} u^{(g_n)} : \hat{\nabla} u^{(g_n)} + \alpha \nabla \cdot u^{(g_n)} \nabla \cdot u^{(g_n)} dx \\
&\quad + \int_{\mathcal{D}} 2(\mu - \mu_0) \hat{\nabla} u^{(g_n)} : \hat{\nabla} u^{(g_n)} + (\lambda - \lambda_0) \nabla \cdot u^{(g_n)} \nabla \cdot u^{(g_n)} dx \\
&\rightarrow -\infty,
\end{aligned}$$

and hence

$$\Lambda(\lambda_0 + \alpha\chi_{\mathcal{B}}, \mu_0 + \beta\chi_{\mathcal{B}}) \not\leq \Lambda(\lambda, \mu).$$

□

In addition, we state the theorem for the case $\lambda \leq \lambda_0$, $\mu \leq \mu_0$.

Theorem 2.2 *Let $(\lambda, \mu) \in L^\infty(\Omega) \times C^{0,1}(\Omega)$ and $\lambda \leq \lambda_0$, $\mu \leq \mu_0$. For every open set \mathcal{B} (e.g. ball or cube) and every $\alpha, \beta \geq 0$, $\alpha + \beta > 0$,*

$$\alpha\chi_{\mathcal{B}} \leq \lambda_0 - \lambda, \quad \beta\chi_{\mathcal{B}} \leq \mu_0 - \mu$$

implies

$$\Lambda(\lambda_0 - \alpha\chi_{\mathcal{B}}, \mu_0 - \beta\chi_{\mathcal{B}}) \leq \Lambda(\lambda, \mu)$$

and

$$\mathcal{B} \not\subseteq \mathcal{D}$$

implies

$$\Lambda(\lambda_0 - \alpha\chi_{\mathcal{B}}, \mu_0 - \beta\chi_{\mathcal{B}}) \not\leq \Lambda(\lambda, \mu).$$

Hence, the set

$$R := \bigcup_{\alpha, \beta \geq 0, \alpha + \beta > 0} \{\mathcal{B} \subseteq \Omega : \Lambda(\lambda_0 - \alpha\chi_{\mathcal{B}}, \mu_0 - \beta\chi_{\mathcal{B}}) \leq \Lambda(\lambda, \mu)\},$$

fulfills

$$\text{inn supp}((\lambda_0 - \lambda, \mu_0 - \mu)^T) \subseteq R \subseteq \mathcal{D}.$$

Proof The proof follows the lines of the proof of Theorem 2.1. □

Based on this, we introduce the monotonicity tests.

Corollary 2.2 *Standard monotonicity test: 1. version*

Let $\lambda_0, \lambda_1, \mu_0, \mu_1 \in \mathbb{R}^+$, $(\lambda, \mu) = (\lambda_0 + (\lambda_1 - \lambda_0)\chi_{\mathcal{D}}, \mu_0 + (\mu_1 - \mu_0)\chi_{\mathcal{D}})$ with $\lambda_1 > \lambda_0$ and $\mu_1 > \mu_0$, where the inclusion \mathcal{D} is open and $\bar{\mathcal{D}} \subset \Omega$ has a connected complement. Further on, let $\alpha, \beta \geq 0$, $\alpha + \beta > 0$ with $\alpha \leq \lambda_1 - \lambda_0$, $\beta \leq \mu_1 - \mu_0$. Then for every open set $\mathcal{B} \subseteq \Omega$

$$\mathcal{B} \subseteq \mathcal{D} \quad \text{if and only if} \quad \Lambda(\lambda_0 + \alpha\chi_{\mathcal{B}}, \mu_0 + \beta\chi_{\mathcal{B}}) \geq \Lambda(\lambda, \mu). \quad (14)$$

Proof Let $\mathcal{B} \subseteq \mathcal{D}$ and $\alpha \leq \lambda_1 - \lambda_0$, $\beta \leq \mu_1 - \mu_0$. This means, that the conditions $\alpha\chi_{\mathcal{B}} \leq \lambda - \lambda_0$, $\beta\chi_{\mathcal{B}} \leq \mu - \mu_0$ of Theorem 2.1 are fulfilled which immediately leads to $\Lambda(\lambda_0 + \alpha\chi_{\mathcal{B}}, \mu_0 + \beta\chi_{\mathcal{B}}) \geq \Lambda(\lambda, \mu)$.

For the opposite direction we assume that there exists a $\mathcal{B} \not\subseteq \mathcal{D}$, which fulfills $\Lambda(\lambda_0 + \alpha\chi_{\mathcal{B}}, \mu_0 + \beta\chi_{\mathcal{B}}) \geq \Lambda(\lambda, \mu)$. By applying the second part of Theorem 2.1 we obtain $\Lambda(\lambda_0 + \alpha\chi_{\mathcal{B}}, \mu_0 + \beta\chi_{\mathcal{B}}) \not\geq \Lambda(\lambda, \mu)$ which contradicts $\Lambda(\lambda_0 + \alpha\chi_{\mathcal{B}}, \mu_0 + \beta\chi_{\mathcal{B}}) \geq \Lambda(\lambda, \mu)$. Hence, $\Lambda(\lambda_0 + \alpha\chi_{\mathcal{B}}, \mu_0 + \beta\chi_{\mathcal{B}}) \geq \Lambda(\lambda, \mu)$ implies that $\mathcal{B} \subseteq \mathcal{D}$. \square

Further on, we formulate the corresponding corollary for the case $\lambda \leq \lambda_0$ and $\mu \leq \mu_0$.

Corollary 2.3 *Standard monotonicity test: 2. version*

Let $\lambda_0, \lambda_1, \mu_0, \mu_1 \in \mathbb{R}^+$, $(\lambda, \mu) = (\lambda_0 + (\lambda_1 - \lambda_0)\chi_{\mathcal{D}}, \mu_0 + (\mu_1 - \mu_0)\chi_{\mathcal{D}})$ with $\lambda_1 < \lambda_0$ and $\mu_1 < \mu_0$, where the inclusion \mathcal{D} is open and $\overline{\mathcal{D}} \subset \Omega$ has a connected complement. Further on, let $\alpha, \beta \geq 0$, $\alpha + \beta > 0$ with $\alpha \leq \lambda_0 - \lambda_1$, $\beta \leq \mu_0 - \mu_1$. Then for every open set $\mathcal{B} \subseteq \Omega$

$$\mathcal{B} \subseteq \mathcal{D} \quad \text{if and only if} \quad \Lambda(\lambda_0 - \alpha\chi_{\mathcal{B}}, \mu_0 - \beta\chi_{\mathcal{B}}) \leq \Lambda(\lambda, \mu). \quad (15)$$

Proof The proof follows the lines of the proof of Corollary 2.2 but we have to consider Theorem 2.2, where $\alpha\chi_{\mathcal{B}} \leq \lambda_0 - \lambda$, $\beta\chi_{\mathcal{B}} \leq \mu_0 - \mu$ implies $\Lambda(\lambda_0 - \alpha\chi_{\mathcal{B}}, \mu_0 - \beta\chi_{\mathcal{B}}) \leq \Lambda(\lambda, \mu)$. Further on, we use that $\mathcal{B} \not\subseteq \mathcal{D}$ implies $\Lambda(\lambda_0 - \alpha\chi_{\mathcal{B}}, \mu_0 - \beta\chi_{\mathcal{B}}) \not\leq \Lambda(\lambda, \mu)$. \square

Next, we apply Theorem 2.1 to difference measurements

$$\Lambda_{\mathcal{D}} = \Lambda(\lambda_0, \mu_0) - \Lambda(\lambda, \mu) \quad (16)$$

which leads directly to the following lemma.

Lemma 2.3 *Let $\Lambda_{\mathcal{B}} = \Lambda(\lambda_0, \mu_0) - \Lambda(\lambda_0 + \alpha\chi_{\mathcal{B}}, \mu_0 + \beta\chi_{\mathcal{B}})$. Under the same assumptions on λ and μ as in Theorem 2.1, we have for every open set \mathcal{B} (e.g. ball or cube) and every $\alpha, \beta \geq 0$, $\alpha + \beta > 0$,*

$$\alpha\chi_{\mathcal{B}} \leq \lambda - \lambda_0, \quad \beta\chi_{\mathcal{B}} \leq \mu - \mu_0 \quad (17)$$

implies

$$\Lambda_{\mathcal{D}} - \Lambda_{\mathcal{B}} \geq 0 \quad (18)$$

and

$$\mathcal{B} \not\subseteq \mathcal{D}$$

implies

$$\Lambda_{\mathcal{D}} - \Lambda_{\mathcal{B}} \not\geq 0.$$

Proof We take a look at the difference $\Lambda_{\mathcal{D}} - \Lambda_{\mathcal{B}} = \Lambda(\lambda_0 + \alpha\chi_{\mathcal{B}}, \mu_0 + \beta\chi_{\mathcal{B}}) - \Lambda(\lambda, \mu)$. The assumption $\alpha\chi_{\mathcal{B}} \leq \lambda - \lambda_0$, $\beta\chi_{\mathcal{B}} \leq \mu - \mu_0$ leads via Theorem 2.1 directly to the desired results. \square

Next, we go over to the consideration of noisy difference measurements

$$\Lambda^\delta \approx \Lambda_{\mathcal{D}} \quad (19)$$

with

$$\|\Lambda^\delta - \Lambda_{\mathcal{D}}\| \leq \delta, \quad (20)$$

where $\delta > 0$ and formulate a monotonicity test (c.f. Corollary 2.2). We have to be aware of the fact that (18) will not hold in general for all $\mathcal{B} \subseteq \mathcal{D}$. Thus, we have to modify the testing in the following way.

Corollary 2.4 *Standard monotonicity test for noisy difference measurements*

Let $\lambda_0, \lambda_1, \mu_0, \mu_1 \in \mathbb{R}^+$, $(\lambda, \mu) = (\lambda_0 + (\lambda_1 - \lambda_0)\chi_{\mathcal{D}}, \mu_0 + (\mu_1 - \mu_0)\chi_{\mathcal{D}})$ with $\lambda_1 > \lambda_0$ and $\mu_1 > \mu_0$, where the inclusion \mathcal{D} is open and $\overline{\mathcal{D}} \subset \Omega$ has a connected complement. Further on, let $\alpha, \beta \geq 0$, $\alpha + \beta > 0$ with $\alpha \leq \lambda_1 - \lambda_0$, $\beta \leq \mu_1 - \mu_0$. Then for noisy data Λ^δ with

$$\|\Lambda^\delta - \Lambda_{\mathcal{D}}\| \leq \delta,$$

and every open set $\mathcal{B} \subseteq \Omega$ we mark \mathcal{B} as inside the inclusion \mathcal{D} only if

$$\Lambda^\delta - \Lambda_{\mathcal{B}} + \delta I \geq 0 \text{ for } \delta > 0 \text{ sufficiently small.}$$

Proof We base our considerations on Remark 3.5 from [13] which deals with the handling of noisy data. Monotonicity tests for noisy difference measurements can be stably implemented in the following sense. Let

$$\|\Lambda^\delta - \Lambda_{\mathcal{D}}\| \leq \delta. \quad (21)$$

By replacing $\Lambda^\delta - \Lambda_{\mathcal{B}}$ by its symmetric part, e.g. by $((\Lambda^\delta - \Lambda_{\mathcal{B}}) + (\Lambda^\delta - \Lambda_{\mathcal{B}})^*)/2$, without loss of generality, we can assume that $\Lambda^\delta - \Lambda_{\mathcal{B}}$ is self-adjoint. Hence, we have for $\Lambda_{\mathcal{D}} - \Lambda_{\mathcal{B}} \geq 0$, that

$$\langle g, (\Lambda^\delta - \Lambda_{\mathcal{B}})g \rangle \geq -\delta \|g\|_{L^2(\Gamma_{\mathcal{N}})^d}$$

for all boundary loads $g \in L^2(\Gamma_{\mathcal{N}})^d$. Thus,

$$\Lambda^\delta - \Lambda_{\mathcal{B}} \geq -\delta I$$

holds in the quadratic sense. If $\Lambda_{\mathcal{D}} - \Lambda_{\mathcal{B}} \not\geq 0$, then $\Lambda_{\mathcal{D}} - \Lambda_{\mathcal{B}}$ has a negative eigenvalue $\theta < 0$, so that

$$\langle g, (\Lambda^\delta - \Lambda_{\mathcal{B}})g \rangle \geq -\delta \|g\|_{L^2(\Gamma_{\mathcal{N}})^d}$$

cannot hold for all $g \in L^2(\Gamma_{\mathcal{N}})^d$ and for $\delta \leq \frac{|\theta|}{2}$. Hence, we mark \mathcal{B} as inside the inclusion \mathcal{D} only if $\Lambda^\delta - \Lambda_{\mathcal{B}} + \delta I \geq 0$ for $0 \leq \delta < \frac{|\theta|}{2}$. \square

2.2. Numerical realization

In order to close this subsection, we take a look at the numerical realization of the monotonicity test (Corollary 2.4) implemented with COMSOL Multiphysics with LiveLink for MATLAB.

Implementation

We are given discrete noisy difference measurements $\bar{\Lambda}^\delta$ which fulfill

$$\|\bar{\Lambda}^\delta - \bar{\Lambda}_D\| \leq \delta, \quad (22)$$

where the notation

$$\bar{A} := (\langle g_i, Ag_j \rangle)_{i,j=1}^m \quad (23)$$

represents the discretized operator corresponding to $A \in \mathcal{L}(L^2(\Gamma_N)^d)$ w.r.t. the boundary loads $g_i \in G$. Here, the set $G := \{g_1, g_2, \dots, g_m\}$ is a system of boundary loads g_i , in which the boundary loads g_i and g_j ($i \neq j$) are pairwise orthogonal.

Let (λ_0, μ_0) be the Lamé parameters of the background material and (λ_1, μ_1) be the Lamé parameters of the inclusion, so that

$$\lambda = \begin{cases} \lambda_0, & x \in \Omega \setminus \mathcal{D}, \\ \lambda_1, & x \in \mathcal{D}, \end{cases} \quad (24)$$

$$\mu = \begin{cases} \mu_0, & x \in \Omega \setminus \mathcal{D}, \\ \mu_1, & x \in \mathcal{D}, \end{cases} \quad (25)$$

$$\tilde{\lambda}_k = \begin{cases} \lambda_0, & x \in \Omega \setminus \mathcal{B}_k, \\ \lambda_0 + \alpha, & x \in \mathcal{B}_k, \end{cases} \quad (26)$$

$$\tilde{\mu}_k = \begin{cases} \mu_0, & x \in \Omega \setminus \mathcal{B}_k, \\ \mu_0 + \beta, & x \in \mathcal{B}_k, \end{cases} \quad (27)$$

where \mathcal{D} denotes the inclusion to be detected and \mathcal{B}_k are $k = 1, \dots, n$ known test inclusions. In addition, the contrasts must fulfill $\alpha \leq \lambda_1 - \lambda_0$ and $\beta \leq \mu_1 - \mu_0$.

For our numerical experiments, we simulate these discrete measurements by solving

$$\left\{ \begin{array}{l} -\mu_0 \Delta u_0 - (\lambda_0 + \mu_0) \nabla(\nabla \cdot u_0) = 0 \quad \text{in } \Omega, \\ -\mu \Delta v - (\lambda + \mu) \nabla(\nabla \cdot v) + ((\mu_1 - \mu_0) \chi_D) \Delta u_0 \\ \quad + ((\lambda_1 - \lambda_0) \chi_D + (\mu_1 - \mu_0) \chi_D) \nabla(\nabla \cdot u_0) = 0 \quad \text{in } \Omega, \\ \left(\lambda_0 (\nabla \cdot u_0) I + 2\mu_0 \hat{\nabla} u_0 \right) n = g_i \quad \text{on } \Gamma_N, \\ \left(\lambda (\nabla \cdot v) I + 2\mu \hat{\nabla} v \right) n = 0 \quad \text{on } \Gamma_N, \\ u_0 = 0 \quad \text{on } \Gamma_D, \\ v = 0 \quad \text{on } \Gamma_D, \end{array} \right. \quad (28)$$

for each of the $i = 1, \dots, m$ boundary loads g_i , where $v := u_0 - u$. The equations regarding v in the system (28) result from subtracting the boundary value problem (1) for the respective Lamé parameters.

To reconstruct the unknown inclusion \mathcal{D} , we determine the Neumann-to-Dirichlet operator for small test cubes \mathcal{B}_k , $k = 1, \dots, n$, so that the Lamé parameters are defined as in

(26) and (27). We calculate

$$\bar{\Lambda}_k := \bar{\Lambda}(\lambda_0, \mu_0) - \bar{\Lambda}(\tilde{\lambda}_k, \tilde{\mu}_k)$$

by solving an analogous system to (28) (but with a different FEM grid to avoid the so-called "inverse crime"). Note that this calculation does not depend on the measurements $\bar{\Lambda}^\delta$ and can be done in advance (in a so-called offline phase). We then compute the eigenvalues of

$$\bar{\Lambda}^\delta - \bar{\Lambda}_k + \delta I.$$

If all eigenvalues are non-negative, then the test cube \mathcal{B}_k is marked as "inside the inclusion".

Results

We present a test model, where we consider a cube of a biological tissue with two inclusions (tumors) as depicted in Figure 2. The Lamé parameters of the corresponding materials are given in Table 1 (see [14]).

material	λ	μ
$x \in \Omega \setminus \mathcal{D}$: tissue	$6.6211 \cdot 10^5$	$6.6892 \cdot 10^3$
$x \in \mathcal{D}$: tumor	$2.3177 \cdot 10^6$	$2.3411 \cdot 10^4$

Table 1. Lamé parameter of the test material in [Pa].

We use the $n = 10 \times 10 \times 10$ test cubes as shown in Figure 2. The face characterized by $z = -0.5$ has zero displacement and each of the other faces is divided in 25 squares of the same size resulting in $m = 125$ patches, where the boundary loads g_i are applied. In this example, the boundary loads g_i are the normal vectors on each patch.

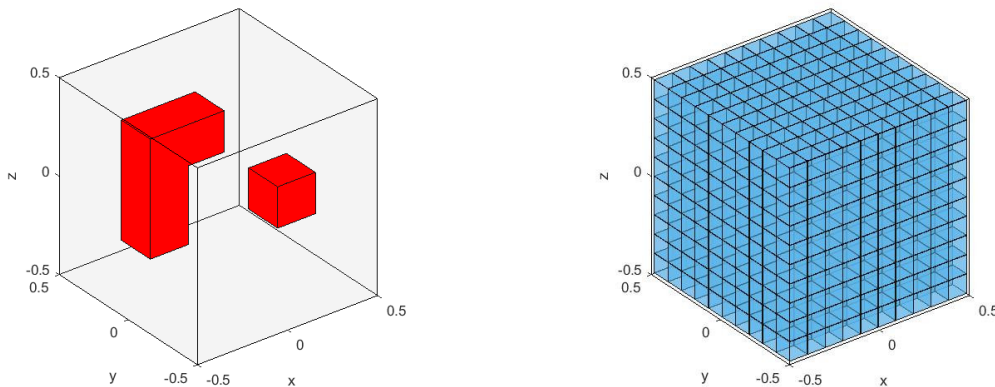


Figure 2. Cube with two inclusions (red, left) and cube with 1000 test blocks (blue, right).

By performing the procedure described before without noise and using the parameters as given in Table 2, we end up with the result in Figure 3, depicting the test blocks with positive eigenvalues marked in red.

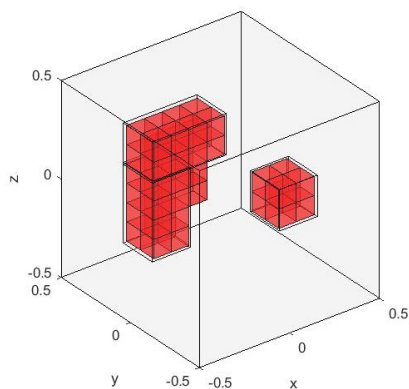


Figure 3. Shape reconstruction of two inclusions (red) via 1000 test cubes for $\alpha = (\lambda_1 - \lambda_0) \approx 16.5 \cdot 10^5 \text{Pa}$, $\beta = (\mu_1 - \mu_0) \approx 16.7 \cdot 10^3 \text{Pa}$ without noise and $\delta = 0$.

We can see that the inclusions are detected correctly and a clear separation of the two inclusions is obtained. However, additional blocks were wrongly detected as lying inside the inclusions.

Further on, we slightly change the setting and take a look at test cubes with the same size as in the first example (see Figure 2). However, now we shift these test cubes so that they do not “perfectly fit” into the unknown inclusions as shown in Figure 4.

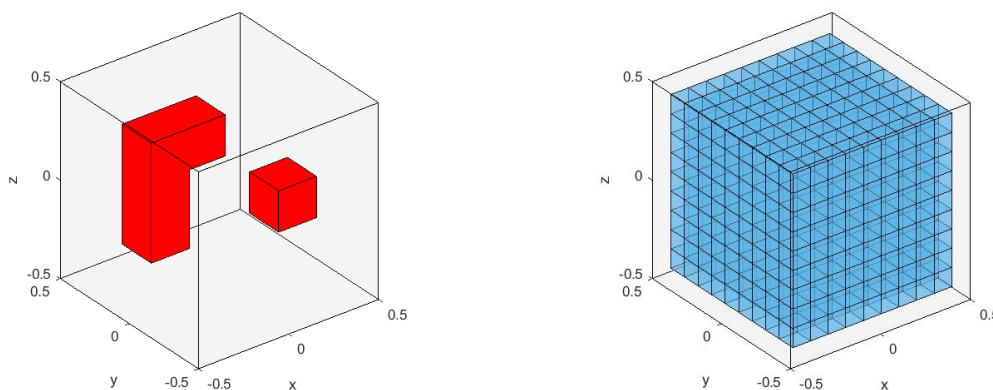


Figure 4. Cube with two inclusions (red, left) and cube with 729 test blocks (blue, right).

Figure 5 depicts the reconstruction of the two inclusions, which are detected but there are also blocks in between wrongly marked.

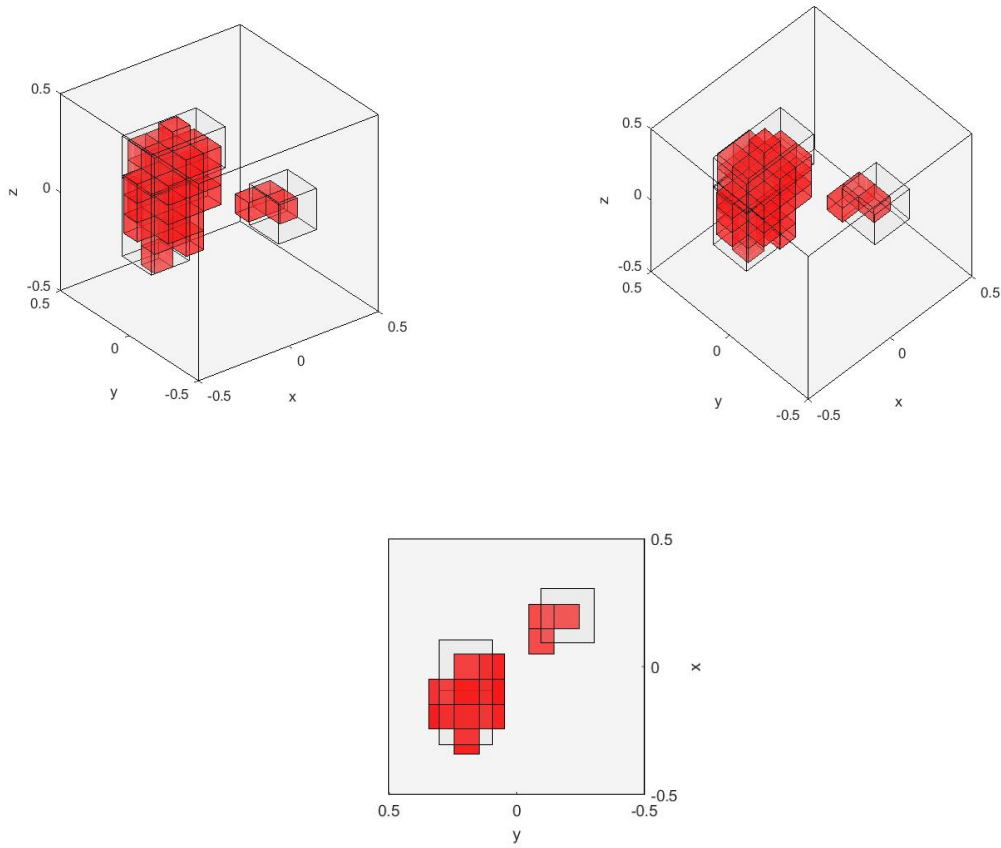


Figure 5. Shape reconstruction of two inclusions (red) via 729 test cubes for $\alpha = (\lambda_1 - \lambda_0) \approx 16.5 \cdot 10^5 \text{Pa}$, $\beta = (\mu_1 - \mu_0) \approx 16.7 \cdot 10^3 \text{Pa}$ without noise and $\delta = 0$.

Next, we take a look at noisy measurement data $\bar{\Lambda}^\delta$ with a noise level of 0.1% and set

$$\bar{\Lambda}^\delta = \bar{\Lambda} + 10^{-3}(\bar{\Lambda}_{ij}E_{ij})_{i,j=1}^m,$$

where $E \in \mathbb{R}^{m \times m}$ contains randomly distributed entries between -1 and 1 . In doing so, we obtain the reconstruction shown in Figure 6, where we chose $\delta = 3 \cdot 10^{-10}$ heuristically. In addition, we want to remark that this δ seems to be relatively small, if one observes that the absolute value of the largest eigenvalue is approximately of order $7 \cdot 10^{-7}$.

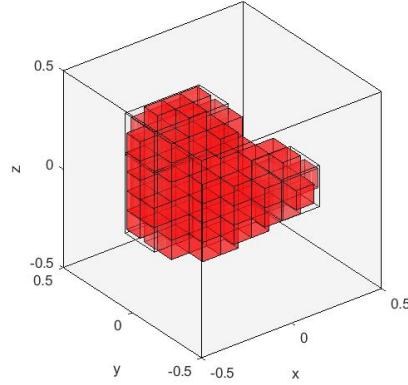


Figure 6. Shape reconstruction of two inclusions (red) via 729 test cubes for $\alpha = (\lambda_1 - \lambda_0) \approx 16.5 \cdot 10^5 \text{Pa}$, $\beta = (\mu_1 - \mu_0) \approx 16.7 \cdot 10^3 \text{Pa}$ with a noise level of 0.1% and $\delta = 3 \cdot 10^{-10}$.

Thus, with a noise level of 0.1% the two inclusions are still located correctly but they are not separated as two single inclusions due to noise.

Remark 2.1 *The main drawback of the method is its offline computation time (see Table 2 in the Appendix) due to the required solutions of problem (28) for each test cube and each Neumann boundary load g_i . However, it should be noted that for testing multiple objects with the same background domain, we only have to perform the offline phase of the test once, since it will be the same for each object to be tested. Hence, in this case, the computation time of the offline phase can be neglected. For testing multiple objects with different background domains, we need a method whose offline computation time is faster. That method is the linearized monotonicity test discussed in the next subsection.*

2.3. Linearized monotonicity method

Now, we go over to the modification of the standard monotonicity method considered so far and introduce the linearized version. For that we apply the Fréchet derivative as defined in (3) in the form

$$\begin{aligned}
 & \langle \Lambda'(\lambda_0, \mu_0)(\alpha\chi_{\mathcal{B}}, \beta\chi_{\mathcal{B}})g, h \rangle & (29) \\
 & = - \int_{\Omega} 2\beta\chi_{\mathcal{B}} \hat{\nabla} u_{(\lambda_0, \mu_0)}^{(g)} : \hat{\nabla} u_{(\lambda_0, \mu_0)}^{(h)} + \alpha\chi_{\mathcal{B}} \nabla \cdot u_{(\lambda_0, \mu_0)}^{(g)} \nabla \cdot u_{(\lambda_0, \mu_0)}^{(h)} dx \\
 & = - \int_{\mathcal{B}} 2\beta \hat{\nabla} u_{(\lambda_0, \mu_0)}^{(g)} : \hat{\nabla} u_{(\lambda_0, \mu_0)}^{(h)} + \alpha \nabla \cdot u_{(\lambda_0, \mu_0)}^{(g)} \nabla \cdot u_{(\lambda_0, \mu_0)}^{(h)} dx.
 \end{aligned}$$

Theorem 2.3 *Let $(\lambda, \mu) \in L^\infty(\Omega) \times C^{0,1}(\Omega)$ and $\lambda \geq \lambda_0$, $\mu \geq \mu_0$. For every open set \mathcal{B} (e.g. ball or cube) and every $\alpha, \beta \geq 0$, $\alpha + \beta > 0$,*

$$\alpha\chi_{\mathcal{B}} \leq \frac{\lambda_0}{\lambda}(\lambda - \lambda_0), \quad \beta\chi_{\mathcal{B}} \leq \frac{\mu_0}{\mu}(\mu - \mu_0)$$

implies

$$\Lambda(\lambda_0, \mu_0) + \Lambda'(\lambda_0, \mu_0)(\alpha\chi_{\mathcal{B}}, \beta\chi_{\mathcal{B}}) \geq \Lambda(\lambda, \mu)$$

and

$$\mathcal{B} \not\subseteq \mathcal{D}$$

implies

$$\Lambda(\lambda_0, \mu_0) + \Lambda'(\lambda_0, \mu_0)(\alpha\chi_{\mathcal{B}}, \beta\chi_{\mathcal{B}}) \not\geq \Lambda(\lambda, \mu).$$

Hence, the set

$$R := \bigcup_{\alpha, \beta \geq 0, \alpha + \beta > 0} \{\mathcal{B} \subseteq \Omega : \Lambda(\lambda_0, \mu_0) + \Lambda'(\lambda_0, \mu_0)(\alpha\chi_{\mathcal{B}}, \beta\chi_{\mathcal{B}}) \geq \Lambda(\lambda, \mu)\}$$

fulfills

$$\text{inn sup}((\lambda - \lambda_0, \mu - \mu_0)^T) \subseteq R \subseteq \mathcal{D}.$$

Proof Let $(\lambda, \mu) \in L^\infty(\Omega) \times C^{0,1}(\Omega)$ and $\lambda \geq \lambda_0, \mu \geq \mu_0$. Let \mathcal{B} be an open set and $\alpha, \beta \geq 0, \alpha + \beta > 0$.

For every $g \in L^2(\Gamma_N)^d$ and solution $u \in \mathcal{V}$ of

$$\begin{cases} -\mu_0 \Delta u - (\lambda_0 + \mu_0) \nabla(\nabla \cdot u) = 0 & \text{in } \Omega, \\ \left(\lambda_0(\nabla \cdot u)I + 2\mu_0 \hat{\nabla} u \right) n = g & \text{on } \Gamma_N, \\ u = 0 & \text{on } \Gamma_D, \end{cases} \quad (30)$$

we have with Lemma 2.2

$$\begin{aligned} & \langle g, (\Lambda(\lambda_0, \mu_0) + \Lambda'(\lambda_0, \mu_0)(\alpha\chi_{\mathcal{B}}, \beta\chi_{\mathcal{B}}) - \Lambda(\lambda, \mu))g \rangle \\ & \geq \int_{\Omega} 2 \left(\frac{\mu_0}{\mu}(\mu - \mu_0) - \beta\chi_{\mathcal{B}} \right) \hat{\nabla} u_{(\lambda_0, \mu_0)} : \hat{\nabla} u_{(\lambda_0, \mu_0)} \\ & \quad + \left(\frac{\lambda_0}{\lambda}(\lambda - \lambda_0) - \alpha\chi_{\mathcal{B}} \right) \nabla \cdot u_{(\lambda_0, \mu_0)} \nabla \cdot u_{(\lambda_0, \mu_0)} dx. \end{aligned}$$

Hence, $\alpha\chi_{\mathcal{B}} \leq \frac{\lambda_0}{\lambda}(\lambda - \lambda_0)$, $\beta\chi_{\mathcal{B}} \leq \frac{\mu_0}{\mu}(\mu - \mu_0)$ implies

$$\Lambda(\lambda_0, \mu_0) + \Lambda'(\lambda_0, \mu_0)(\alpha\chi_{\mathcal{B}}, \beta\chi_{\mathcal{B}}) \geq \Lambda(\lambda, \mu).$$

It remains to show that

$$\mathcal{B} \not\subseteq \mathcal{D} \quad \text{implies} \quad \Lambda(\lambda_0, \mu_0) + \Lambda'(\lambda_0, \mu_0)(\alpha\chi_{\mathcal{B}}, \beta\chi_{\mathcal{B}}) \not\geq \Lambda(\lambda, \mu).$$

Let $\mathcal{B} \not\subseteq \mathcal{D}$. The monotonicity relation from Corollary 2.1 yields that shrinking the open set \mathcal{B} makes $\Lambda(\lambda_0, \mu_0) + \Lambda'(\lambda_0, \mu_0)(\alpha\chi_{\mathcal{B}}, \beta\chi_{\mathcal{B}})$ larger, so we can assume without loss of generality that

$$\mathcal{B} \subset \Omega \setminus \mathcal{D}.$$

Then we obtain in the same way as in the proof of Theorem 2.1 for $u^{(g_n)}$ as in (30)

$$\begin{aligned}
& \langle g_n, (\Lambda(\lambda_0, \mu_0) + \Lambda'(\lambda_0, \mu_0)(\alpha\chi_{\mathcal{B}}, \beta\chi_{\mathcal{B}}) - \Lambda(\lambda, \mu)g_n) \rangle \\
& \leq \int_{\Omega} 2(\mu - (\mu_0 + \beta\chi_{\mathcal{B}})) \hat{\nabla} u_{(\lambda, \mu)}^{(g_n)} : \hat{\nabla} u_{(\lambda, \mu)}^{(g_n)} \\
& \quad + (\lambda - (\lambda_0 + \alpha\chi_{\mathcal{B}})) \nabla \cdot u_{(\lambda, \mu)}^{(g_n)} \nabla \cdot u_{(\lambda, \mu)}^{(g_n)} dx \\
& = - \int_{\mathcal{B}} 2\beta \hat{\nabla} u^{(g_n)} : \hat{\nabla} u^{(g_n)} + \alpha \nabla \cdot u^{(g_n)} \nabla \cdot u^{(g_n)} dx \\
& \quad + \int_{\mathcal{D}} 2(\mu - \mu_0) \hat{\nabla} u^{(g_n)} : \hat{\nabla} u^{(g_n)} + (\lambda - \lambda_0) \nabla \cdot u^{(g_n)} \nabla \cdot u^{(g_n)} dx
\end{aligned}$$

so that the assertion follows using localized potential for the background parameters (μ_0, λ_0) as in Theorem 2.1. \square

Next, we formulate a theorem for the case $\lambda \leq \lambda_0, \mu \leq \mu_0$.

Theorem 2.4 *Let $(\lambda, \mu) \in L^\infty(\Omega) \times C^{0,1}(\Omega)$ and $\lambda \leq \lambda_0, \mu \leq \mu_0$. For every open set \mathcal{B} (e.g. ball or cube) and every $\alpha, \beta \geq 0, \alpha + \beta > 0$,*

$$\alpha\chi_{\mathcal{B}} \leq \lambda_0 - \lambda, \quad \beta\chi_{\mathcal{B}} \leq \mu_0 - \mu$$

implies

$$\Lambda(\lambda_0, \mu_0) - \Lambda'(\lambda_0, \mu_0)(\alpha\chi_{\mathcal{B}}, \beta\chi_{\mathcal{B}}) \leq \Lambda(\lambda, \mu)$$

and

$$\mathcal{B} \not\subseteq \mathcal{D}$$

implies

$$\Lambda(\lambda_0, \mu_0) - \Lambda'(\lambda_0, \mu_0)(\alpha\chi_{\mathcal{B}}, \beta\chi_{\mathcal{B}}) \not\leq \Lambda(\lambda, \mu).$$

Hence, the set

$$R := \bigcup_{\alpha, \beta \geq 0, \alpha + \beta > 0} \{\mathcal{B} \subseteq \Omega : \Lambda(\lambda_0, \mu_0) - \Lambda'(\lambda_0, \mu_0)(\alpha\chi_{\mathcal{B}}, \beta\chi_{\mathcal{B}}) \leq \Lambda(\lambda, \mu)\}$$

fulfills

$$\text{inn supp}((\lambda_0 - \lambda, \mu_0 - \mu)^T) \subseteq R \subseteq \mathcal{D}.$$

Proof In order to prove this theorem, we have to consider the same steps as in the proof of Theorem 2.3, but we have to apply the estimate from Lemma 2.1 instead of Lemma 2.2 which results in different upper bounds on the contrasts α and β . \square

Summarizing the results from Theorem 2.3 as well as Theorem 2.4, we end up with the linearized monotonicity tests as introduced in Corollary 2.5 and 2.6.

Corollary 2.5 *Linearized monotonicity test: 1. version*

Let $\lambda_0, \lambda_1, \mu_0, \mu_1 \in \mathbb{R}^+$, $(\lambda, \mu) = (\lambda_0 + (\lambda_1 - \lambda_0)\chi_{\mathcal{D}}, \mu_0 + (\mu_1 - \mu_0)\chi_{\mathcal{D}})$ with $\lambda_1 > \lambda_0$ and $\mu_1 > \mu_0$, where the inclusion \mathcal{D} is open and $\overline{\mathcal{D}}$ has a connected complement. Further on,

let $\alpha, \beta \geq 0$, $\alpha + \beta > 0$ with $\alpha \leq \frac{\lambda_0}{\lambda_1}(\lambda_1 - \lambda_0)$, $\beta \leq \frac{\mu_0}{\mu_1}(\mu_1 - \mu_0)$. Then for every open set $\mathcal{B} \subseteq \Omega$

$$\mathcal{B} \subseteq \mathcal{D} \quad \text{if and only if} \quad \Lambda(\lambda_0, \mu_0) + \Lambda'(\lambda_0, \mu_0)(\alpha\chi_{\mathcal{B}}, \beta\chi_{\mathcal{B}}) \geq \Lambda(\lambda, \mu).$$

Proof The proof of Corollary 2.5 follows from Theorem 2.3 analogous to the proof of Corollary 2.2. \square

In addition, we formulate the linearized monotonicity test for the case $\lambda \leq \lambda_0$ and $\mu \leq \mu_0$.

Corollary 2.6 *Linearized monotonicity test: 2. version*

Let $\lambda_0, \lambda_1, \mu_0, \mu_1 \in \mathbb{R}^+$, $(\lambda, \mu) = (\lambda_0 + (\lambda_1 - \lambda_0)\chi_{\mathcal{D}}, \mu_0 + (\mu_1 - \mu_0)\chi_{\mathcal{D}})$ with $\lambda_1 < \lambda_0$ and $\mu_1 < \mu_0$, where the inclusion \mathcal{D} is open and $\overline{\mathcal{D}}$ has a connected complement. Further on, let $\alpha, \beta \geq 0$, $\alpha + \beta > 0$ with $\alpha \leq \lambda_0 - \lambda_1$, $\beta \leq \mu_0 - \mu_1$. Then for every open set $\mathcal{B} \subseteq \Omega$

$$\mathcal{B} \subseteq \mathcal{D} \quad \text{if and only if} \quad \Lambda(\lambda_0, \mu_0) - \Lambda'(\lambda_0, \mu_0)(\alpha\chi_{\mathcal{B}}, \beta\chi_{\mathcal{B}}) \leq \Lambda(\lambda, \mu).$$

Proof In order to prove this corollary, we apply the results of Theorem 2.4 in a similar way as in the the proof of Corollary 2.2. \square

Next, we apply Theorem 2.3 to difference measurements $\Lambda_{\mathcal{D}}$ as defined in (16) and obtain the following lemma.

Lemma 2.4 Let $\Lambda'_{\mathcal{B}} = \Lambda'(\lambda_0, \mu_0)(\alpha\chi_{\mathcal{B}}, \beta\chi_{\mathcal{B}})$. Under the same assumptions on λ and μ as in Theorem 2.3, we have for every open set \mathcal{B} (e.g. ball or cube) and every $\alpha, \beta \geq 0$, $\alpha + \beta > 0$,

$$\alpha\chi_{\mathcal{B}} \leq \frac{\lambda_0}{\lambda}(\lambda - \lambda_0), \quad \beta\chi_{\mathcal{B}} \leq \frac{\mu_0}{\mu}(\mu - \mu_0) \quad (31)$$

implies

$$\Lambda_{\mathcal{D}} + \Lambda'_{\mathcal{B}} \geq 0$$

and

$$\mathcal{B} \not\subseteq \mathcal{D}$$

implies

$$\Lambda_{\mathcal{D}} + \Lambda'_{\mathcal{B}} \not\geq 0.$$

Proof Similar as in the proof of Theorem 2.1, we start with the consideration of $\Lambda_{\mathcal{D}} + \Lambda'_{\mathcal{B}} = \Lambda(\lambda_0, \mu_0) - \Lambda(\lambda, \mu) + \Lambda'(\lambda_0, \mu_0)(\alpha\chi_{\mathcal{B}}, \beta\chi_{\mathcal{B}})$ and obtain the corresponding relations with Theorem 2.3. \square

As for the standard monotonicity test, we also introduce a linearized monotonicity test for noisy data (c.f. Corollary 2.5). Let the noisy difference data be given by (19) and fulfill (20).

Corollary 2.7 *Linearized monotonicity test for noisy data*

Let $\lambda_0, \lambda_1, \mu_0, \mu_1 \in \mathbb{R}^+$, $(\lambda, \mu) = (\lambda_0 + (\lambda_1 - \lambda_0)\chi_{\mathcal{D}}, \mu_0 + (\mu_1 - \mu_0)\chi_{\mathcal{D}})$ with $\lambda_1 > \lambda_0$ and $\mu_1 > \mu_0$, where the inclusion \mathcal{D} is open and $\overline{\mathcal{D}}$ has a connected complement. Further on, let $\alpha, \beta \geq 0$, $\alpha + \beta > 0$ with $\alpha \leq \frac{\lambda_0}{\lambda_1}(\lambda_1 - \lambda_0)$, $\beta \leq \frac{\mu_0}{\mu_1}(\mu_1 - \mu_0)$. Then for noisy data Λ^δ with

$$\|\Lambda^\delta - \Lambda_{\mathcal{D}}\| \leq \delta,$$

and every open set $\mathcal{B} \subseteq \Omega$ we mark \mathcal{B} as inside the inclusion \mathcal{D} only if

$$\Lambda^\delta + \Lambda'_{\mathcal{B}} + \delta I \geq 0 \text{ for } \delta > 0 \text{ sufficiently small.}$$

Proof We proceed in a similar as in the proof of Corollary 2.4 and summarize the essential results of that proof. Possibly replacing $\Lambda^\delta + \Lambda'_{\mathcal{B}}$ by its symmetric part we may assume that $\Lambda^\delta + \Lambda'_{\mathcal{B}}$ is self-adjoint. Hence, we have for $\Lambda_{\mathcal{D}} + \Lambda'_{\mathcal{B}} \geq 0$, that

$$\langle g, (\Lambda^\delta + \Lambda'_{\mathcal{B}})g \rangle \geq -\delta \|g\|_{L^2(\Gamma_N)^d}$$

for all boundary loads $g \in L^2(\Gamma_N)^d$, since

$$\Lambda^\delta + \Lambda'_{\mathcal{B}} = \Lambda_{\mathcal{D}} + \Lambda'_{\mathcal{B}} + \Lambda^\delta - \Lambda_{\mathcal{D}} \geq -\delta I.$$

If $\Lambda_{\mathcal{D}} + \Lambda'_{\mathcal{B}} \not\geq 0$, then $\Lambda_{\mathcal{D}} + \Lambda'_{\mathcal{B}}$ has a negative eigenvalue $\theta < 0$, so that

$$\langle g, (\Lambda^\delta + \Lambda'_{\mathcal{B}})g \rangle \geq -\delta \|g\|_{L^2(\Gamma_N)^d}$$

cannot hold for all $g \in L^2(\Gamma_N)^d$ for $\delta \leq \frac{|\theta|}{2}$. Hence, we mark \mathcal{B} as inside the inclusion \mathcal{D} only if $\Lambda^\delta + \Lambda'_{\mathcal{B}} + \delta I \geq 0$ for $0 \leq \delta < \frac{|\theta|}{2}$. \square

2.4. Numerical realization

Next, we go over to the implementation of the linearized monotonicity test according to Corollary 2.7. The implementation is again conducted with COMSOL Multiphysics with LiveLink for MATLAB.

Implementation

In doing so, we solve system (28) to simulate our discrete noisy difference measurements $\overline{\Lambda}^\delta$ which must fulfill

$$\|\overline{\Lambda}^\delta - \overline{\Lambda}\| \leq \delta.$$

With λ, μ as in (24)-(25) and

$$\begin{aligned} \tilde{\lambda}_k &= \alpha \chi_{\mathcal{B}_k}, \\ \tilde{\mu}_k &= \beta \chi_{\mathcal{B}_k}, \end{aligned}$$

where the contrasts must fulfill $\alpha \leq \frac{\lambda_0}{\lambda_1}(\lambda_1 - \lambda_0)$ and $\beta \leq \frac{\mu_0}{\mu_1}(\mu_1 - \mu_0)$, we proceed as follows. To reconstruct the unknown inclusion \mathcal{D} , we determine the Fréchet derivative

$$\overline{\Lambda}'_k := \overline{\Lambda}'(\lambda_0, \mu_0)(\tilde{\lambda}_k, \tilde{\mu}_k)$$

for each of the test cubes \mathcal{B}_k , $k = 1, \dots, n$, by an approximation via Gaussian quadrature in MATLAB. The required solution u_0 for the background Lamé parameters used in the calculation of $\overline{\Lambda}'_k$ is again calculated via COMSOL.

Note that this calculation does not depend on the measurements Λ^δ and can be done in advance (in a so-called offline phase).

We then estimate the eigenvalues of

$$\overline{\Lambda}^\delta + \overline{\Lambda}'_k + \delta I.$$

If all eigenvalues are non-negative, then the test cube \mathcal{B}_k is marked as "inside the inclusion".

Results

First, we consider the same setting as for the standard monotonicity method. Implementing the linearized monotonicity method for the same boundary loads g_i and without noise leads to the result depicted in Figure 7, where the test cubes with positive eigenvalues are marked in red. The computation time as well as the applied parameters can again be found in the Appendix (Table 2).

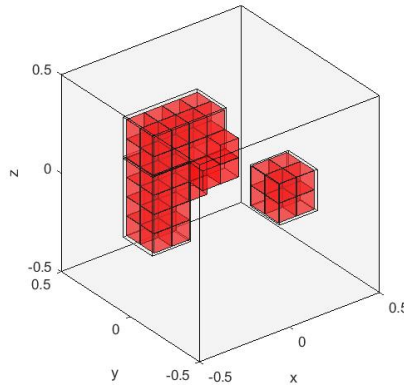


Figure 7. Shape reconstruction of two inclusions (red) via 1000 test cubes for $\alpha = 0.28(\lambda_1 - \lambda_0) \approx 4.6 \cdot 10^5 \text{ Pa}$, $\beta = 0.28(\mu_1 - \mu_0) \approx 4.7 \cdot 10^3 \text{ Pa}$ without noise and $\delta = 0$.

As a result, we get a similar outcome as we obtained with the non-linearized monotonicity tests (for comparison see Figure 3). However, the result for the non-linearized monotonicity method is slightly better. The reason is the stronger constraint on α and β in the non-linearized case (c.f. Equations (17) and (31)). In other words, the non-linearized method allows us to test with stronger contrasts.

Remark 2.2 *All in all, the complete computation time including the offline phase for the linearized monotonicity test is faster (cf. Table 2). However, the direct and the online time are similar if one uses the same mesh size. Hence, for testing objects with different background domains, the linearized approach should be applied since the offline phase has to be realized each time. For testing many objects with the same background domain, the non-linearized method should be applied, since it provides a slightly more precise reconstruction. The drawback of the offline calculation time is mitigated in this case, since it has to be calculated only once at the beginning, so that the testing itself for each object is as fast as the testing via the linearized method without its offline phase.*

The significantly shorter offline phase of the linearized monotonicity method (see Table 2), allows us to increase the number of test blocks. In addition, we also increase the number of tetrahedrons to test the influence of the mesh size on the runtime and in order to provide enough nodes inside of the smaller test blocks so that the Fréchet derivative can be calculated with sufficient precision. Hence, we go over to a slightly different setting (Figure 8), where we perform the testing for 125 patches with $14 \times 14 \times 14$ test cubes instead of $10 \times 10 \times 10$ cubes in order to obtain a higher resolution. We want to remark that these smaller cubes are chosen in such a way that some of them are also lying on the boundary of the inclusions we want to detect. That means, that in theory, we are able to detect also smaller inclusions than the test cubes used before and a higher resolution enables us to reconstruct inclusions, which do not surround a complete test block for a coarser set of test blocks, since Theorem 2.3 guarantees that we cannot detect inclusions smaller than the used test inclusions.

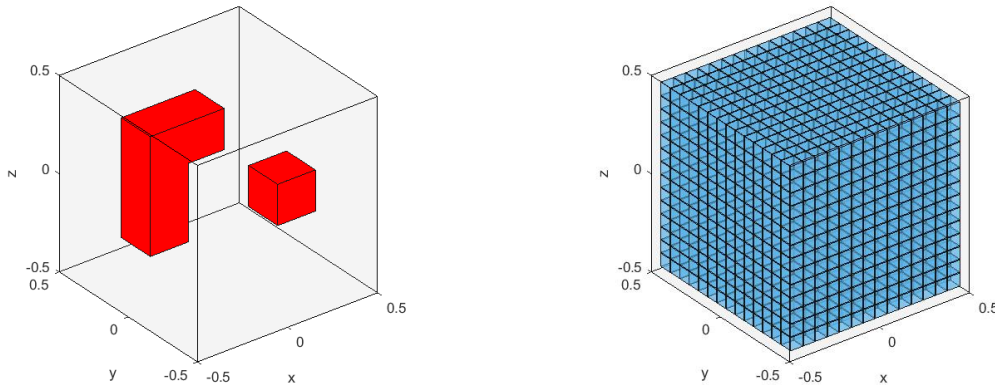


Figure 8. Cube with two inclusions (red, left) and cube with 2744 test blocks (blue, right).

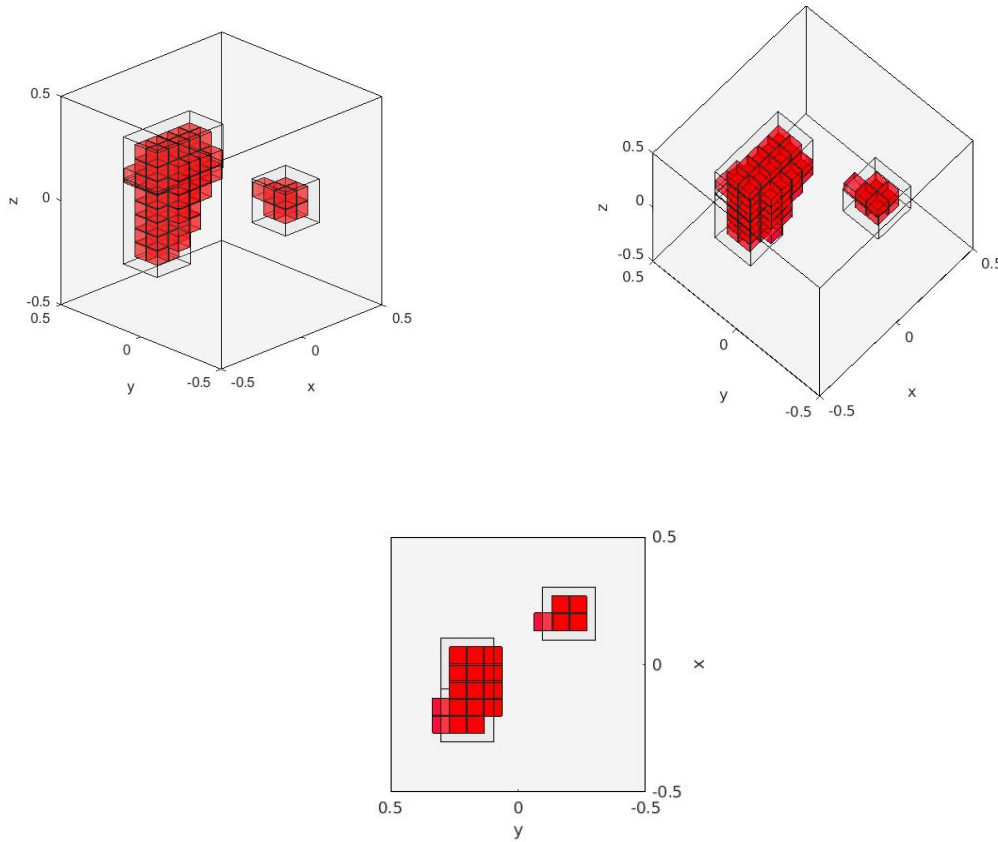


Figure 9. Shape reconstruction of two inclusions (red) via 2744 test cubes for $\alpha = 0.28(\lambda_1 - \lambda_0) \approx 4.6 \cdot 10^5 \text{Pa}$, $\beta = 0.28(\mu_1 - \mu_0) \approx 4.7 \cdot 10^3 \text{Pa}$ without noise and $\delta = 0$.

We see that the two inclusions are detected and their shape is reconstructed almost correctly. However, additional blocks were wrongly detected. Those blocks lie again between the two inclusions, as was the case for the standard monotonicity method, or are only partially located inside of the inclusion.

Remark 2.3 *If we compare the noiseless results of the standard monotonicity method (Figure 5) with the one from the linearized monotonicity method (Figure 9), we can conclude that in our examples with both methods, the inclusions were detected. In addition, our numerical example showed that both monotonicity methods reconstruct the shape of the inclusions and are able to separate them.*

Finally, as for the standard monotonicity method, we again present the result obtained from noisy data Λ^δ with a noise level of 0.1% (Figure 10).

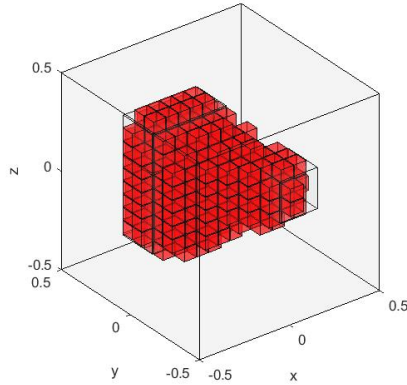


Figure 10. Shape reconstruction of two inclusions (red) via 2744 test cubes for $\alpha = 0.28(\lambda_1 - \lambda_0) \approx 4.6 \cdot 10^5 \text{Pa}$, $\beta = 0.28(\mu_1 - \mu_0) \approx 4.7 \cdot 10^3 \text{Pa}$ with noise level of 0.1% and $\delta = 5 \cdot 10^{-10}$.

This reconstruction shows us that the linearized monotonicity method applied to noisy data gives similar results as the standard monotonicity method (see Figure 6). The inclusion is again located correctly, but a separation is not possible due to the noise level.

3. Conclusion and Outlook

In this paper we introduced and analyzed the standard as well as linearized monotonicity method for the linear elasticity problem and gave an insight into the performance of the monotonicity tests. Further on, we showed numerical examples of the different methods and compared them with each other. The next step will be the adaptation of these methods to the elastic Helmholtz-type equation.

Appendix

The runtime of the two methods are given in Table 2. We distinguish between the solution of the direct and inverse problem, which itself is split into its offline and online phase. The direct problem represents the simulation of the difference measurements, which are provided by a user in practice. For the inverse problem, the offline phase includes the calculation of all quantities which can be computed without knowing the measurements, i.e. all quantities that only depend on (λ_0, μ_0) and are calculated on a different grid as the direct problem to avoid “inverse crime”. Contrary, the online phase includes all computations which depend on the difference measurements.

It should be noted that the approach for the direct problem is the same for the non-linearized and linearized method, so that the computation times are nearly identical for the same grid size (see the two examples for 1000 pixel). As expected, the computation

time increases while increasing the number of tetrahedrons used in the discretization (cf. last line of Table 2). In addition, the offline phase is considerably larger than the runtime of the direct problem. This is due to the computation time of the Fréchet derivative.

runtime	direct problem	inverse problem offline phase	inverse problem online phase
non-linearized method, $\alpha = (\lambda_1 - \lambda_0) \approx 16.5 \cdot 10^5 \text{Pa}$, $\beta = (\mu_1 - \mu_0) \approx 16.7 \cdot 10^3 \text{Pa}$, 1000 pixel, #tetrahedrons = 7644 (direct problem, offline similar)	9min 10s	6d 23h 43min	2min 27s
non-linearized method, $\alpha = (\lambda_1 - \lambda_0) \approx 16.5 \cdot 10^5 \text{Pa}$, $\beta = (\mu_1 - \mu_0) \approx 16.7 \cdot 10^3 \text{Pa}$, 729 pixel, #tetrahedrons = 7644 (direct problem, offline similar)	9min 23s	4d 20h 54min	2min 37s
linearized method, $\alpha = 0.28(\lambda_1 - \lambda_0) \approx 4.6 \cdot 10^5 \text{Pa}$, $\beta = 0.28(\mu_1 - \mu_0) \approx 4.7 \cdot 10^3 \text{Pa}$, 1000 pixel, #tetrahedrons = 7644 (direct problem, offline similar)	9min 13s	1h 3min 52s	2min 12s
linearized method, $\alpha = 0.28(\lambda_1 - \lambda_0) \approx 4.6 \cdot 10^5 \text{Pa}$, $\beta = 0.28(\mu_1 - \mu_0) \approx 4.7 \cdot 10^3 \text{Pa}$, 2744 pixel, #tetrahedrons = 37252 (direct problem, offline similar)	1h 4min	6h 40min	7min 39s

Table 2. Comparison of the standard (non-linearized) and linearized monotonicity method.

References

- [1] E. Beretta, E. Francini, A. Morassi, E. Rosset, and S. Vessella. Lipschitz continuous dependence of piecewise constant Lamé coefficients from boundary data: the case of non-flat interfaces. *Inverse Problems*, 30(12):125005, 2014.
- [2] E. Beretta, E. Francini, and S. Vessella. Uniqueness and Lipschitz stability for the identification of Lamé parameters from boundary measurements. *Inverse Problems & Imaging*, 8(3):611–644, 2014.
- [3] P. G. Ciarlet. *The finite element method for elliptic problems*. North Holland, 1978.
- [4] S. Eberle, B. Harrach, H. Meftahi, and T. Rezgui. Lipschitz stability estimate and reconstruction of Lamé parameters in linear elasticity. *arXiv preprint: arXiv:1906.02194*, 2019.
- [5] G. Eskin and J. Ralston. On the inverse boundary value problem for linear isotropic elasticity. *Inverse Problems*, 18(3):907, 2002.

- [6] K. O. Friedrichs. On the boundary-value problems of elasticity and Korn's inequality. *Annals of Mathematics*, 48:441–471, 1947.
- [7] B. Gebauer. Localized potentials in electrical impedance tomography. *Inverse Probl. Imaging*, 2(2):251–269, 2008.
- [8] B. Harrach. On uniqueness in diffuse optical tomography. *Inverse problems*, 25(5):055010, 2009.
- [9] B. Harrach. Simultaneous determination of the diffusion and absorption coefficient from boundary data. *Inverse Probl. Imaging*, 6(4):663–679, 2012.
- [10] B. Harrach. Recent progress on the factorization method for electrical impedance tomography. *Comput. Math. Methods Med.*, vol. 2013, Article ID 425184, 8 pages, 2013.
- [11] B. Harrach, Y.-H. Lin, and H. Liu. On localizing and concentrating electromagnetic fields. *SIAM J. Appl. Math.*, 78(5):2558–2574, 2018.
- [12] B. Harrach, V. Pohjola, and M. Salo. Monotonicity and local uniqueness for the Helmholtz equation. *Anal. PDE*, 12(7):1741–1771, 2019.
- [13] B. Harrach and M. Ullrich. Monotonicity-based shape reconstruction in electrical impedance tomography. *SIAM Journal on Mathematical Analysis*, 45(6):3382–3403, 2013.
- [14] K. M. Hiltawsky. *Analyse und Optimierung von Abbildungseigenschaften der Ultraschall-Elastographie*. PhD thesis, Ruhr-Universität Bochum, 2004.
- [15] M. Ikehata. Inversion formulas for the linearized problem for an inverse boundary value problem in elastic prospection. *SIAM Journal on Applied Mathematics*, 50(6):1635–1644, 1990.
- [16] O. Y. Imanuvilov and M. Yamamoto. On reconstruction of Lamé coefficients from partial Cauchy data. *Journal of Inverse and Ill-posed Problems*, 19(6):881–891, 2011.
- [17] A. Lechleiter, N. Hyvönen, and H. Hakula. The factorization method applied to the complete electrode model of impedance tomography. *SIAM J. Appl. Math.*, 68:1097–1121, 2008.
- [18] Y.-H. Lin and G. Nakamura. Boundary determination of the Lamé moduli for the isotropic elasticity system. *Inverse Problems*, 33(12):125004, 2017.
- [19] G. Nakamura, K. Tanuma, and G. Uhlmann. Layer stripping for a transversely isotropic elastic medium. *SIAM Journal on Applied Mathematics*, 59(5):1879–1891, 1999.
- [20] G. Nakamura and G. Uhlmann. Identification of Lamé parameters by boundary measurements. *American Journal of Mathematics*, pages 1161–1187, 1993.
- [21] G. Nakamura and G. Uhlmann. Inverse problems at the boundary for an elastic medium. *SIAM journal on mathematical analysis*, 26(2):263–279, 1995.
- [22] G. Nakamura and G. Uhlmann. Global uniqueness for an inverse boundary value problem arising in elasticity. *Inventiones mathematicae*, 152(1):205–207, 2003.
- [23] A. Tamburrino. Monotonicity based imaging methods for elliptic and parabolic inverse problems. *J. Inverse Ill-Posed Probl.*, 14(6):633–642, 2006.
- [24] A. Tamburrino and G. Rubinacci. A new non-iterative inversion method for electrical resistance tomography. *Inverse Problems*, 18(6):1809, 2002.